ISSN 1726-5479

SENSORS & TRANSDUCERS

10/12 vol. 15 Special

MEMS & NEMS Sensors

International Frequency Sensor Association Publishing

Sensors & Transducers

Volume 15, Special Issue
October 2012
www.sensorsportal.com
ISSN 1726-5479

Editors-in-Chief: professor Sergey Y. Yurish, tel.: +34 696067716, e-mail: editor@sensorsportal.com

Editors for Western Europe
Meijer, Gerard C.M., Delft University of Technology, The Netherlands
Ferrari, Vittorio, Universitá di Brescia, Italy

Editors for North America
Datskos, Panos G., Oak Ridge National Laboratory, USA
Fabien, J. Josse, Marquette University, USA
Katz, Evgeny, Clarkson University, USA

Editor South America
Costa-Felix, Rodrigo, Inmetro, Brazil

Editor for Eastern Europe
Sachenko, Anatoly, Ternopil State Economic University, Ukraine

Editor for Asia
Ohyama, Shinji, Tokyo Institute of Technology, Japan

Editor for Africa
Maki K.Habib, American University in Cairo, Egypt

Editor for Asia-Pacific
Mukhopadhyay, Subhas, Massey University, New Zealand

Editorial Advisory Board

Abdul Rahim, Ruzairi, Universiti Teknologi, Malaysia
Ahmad, Mohd Noor, Nothern University of Engineering, Malaysia
Annamalai, Karthigeyan, National Institute of Advanced Industrial Science and Technology, Japan
Arcega, Francisco, University of Zaragoza, Spain
Arguel, Philippe, CNRS, France
Ahn, Jae-Pyoung, Korea Institute of Science and Technology, Korea
Arndt, Michael, Robert Bosch GmbH, Germany
Ascoli, Giorgio, George Mason University, USA
Atalay, Selcuk, Inonu University, Turkey
Atghiaee, Ahmad, University of Tehran, Iran
Augutis, Vygantas, Kaunas University of Technology, Lithuania
Avachit, Patil Lalchand, North Maharashtra University, India
Ayesh, Aladdin, De Montfort University, UK
Azamimi, Azian binti Abdullah, Universiti Malaysia Perlis, Malaysia
Bahreyni, Behraad, University of Manitoba, Canada
Baliga, Shankar, B., General Monitors Transnational, USA
Baoxian, Ye, Zhengzhou University, China
Barford, Lee, Agilent Laboratories, USA
Barlingay, Ravindra, RF Arrays Systems, India
Basu, Sukumar, Jadavpur University, India
Beck, Stephen, University of Sheffield, UK
Ben Bouzid, Sihem, Institut National de Recherche Scientifique, Tunisia
Benachaiba, Chellali, Universitaire de Bechar, Algeria
Binnie, T. David, Napier University, UK
Bischoff, Gerlinde, Inst. Analytical Chemistry, Germany
Bodas, Dhananjay, IMTEK, Germany
Borges Carval, Nuno, Universidade de Aveiro, Portugal
Bouchikhi, Benachir, University Moulay Ismail, Morocco
Bousbia-Salah, Mounir, University of Annaba, Algeria
Bouvet, Marcel, CNRS – UPMC, France
Brudzewski, Kazimierz, Warsaw University of Technology, Poland
Cai, Chenxin, Nanjing Normal University, China
Cai, Qingyun, Hunan University, China
Calvo-Gallego, Jaime, Universidad de Salamanca, Spain
Campanella, Luigi, University La Sapienza, Italy
Carvalho, Vitor, Minho University, Portugal
Cecelja, Franjo, Brunel University, London, UK
Cerda Belmonte, Judith, Imperial College London, UK
Chakrabarty, Chandan Kumar, Universiti Tenaga Nasional, Malaysia
Chakravorty, Dipankar, Association for the Cultivation of Science, India
Changhai, Ru, Harbin Engineering University, China
Chaudhari, Gajanan, Shri Shivaji Science College, India
Chavali, Murthy, N.I. Center for Higher Education, (N.I. University), India
Chen, Jiming, Zhejiang University, China
Chen, Rongshun, National Tsing Hua University, Taiwan
Cheng, Kuo-Sheng, National Cheng Kung University, Taiwan
Chiang, Jeffrey (Cheng-Ta), Industrial Technol. Research Institute, Taiwan
Chiriac, Horia, National Institute of Research and Development, Romania
Chowdhuri, Arijit, University of Delhi, India
Chung, Wen-Yaw, Chung Yuan Christian University, Taiwan
Corres, Jesus, Universidad Publica de Navarra, Spain
Cortes, Camilo A., Universidad Nacional de Colombia, Colombia
Courtois, Christian, Universite de Valenciennes, France
Cusano, Andrea, University of Sannio, Italy
D'Amico, Arnaldo, Università di Tor Vergata, Italy
De Stefano, Luca, Institute for Microelectronics and Microsystem, Italy
Deshmukh, Kiran, Shri Shivaji Mahavidyalaya, Barshi, India
Dickert, Franz L., Vienna University, Austria
Dieguez, Angel, University of Barcelona, Spain
Dighavkar, C. G., M.G. Vidyamandir's L. V.H. College, India
Dimitropoulos, Panos, University of Thessaly, Greece
Ding, Jianning, Jiangsu Polytechnic University, China
Djordjevich, Alexandar, City University of Hong Kong, Hong Kong
Donato, Nicola, University of Messina, Italy
Donato, Patricio, Universidad de Mar del Plata, Argentina
Dong, Feng, Tianjin University, China
Drljaca, Predrag, Instersema Sensoric SA, Switzerland
Dubey, Venketesh, Bournemouth University, UK
Enderle, Stefan, Univ.of Ulm and KTB Mechatronics GmbH, Germany
Erdem, Gursan K. Arzum, Ege University, Turkey
Erkmen, Aydan M., Middle East Technical University, Turkey
Estelle, Patrice, Insa Rennes, France
Estrada, Horacio, University of North Carolina, USA
Faiz, Adil, INSA Lyon, France
Fericean, Sorin, Balluff GmbH, Germany
Fernandes, Joana M., University of Porto, Portugal
Francioso, Luca, CNR-IMM Institute for Microelectronics and Microsystems, Italy
Francis, Laurent, University Catholique de Louvain, Belgium
Fu, Weiling, South-Western Hospital, Chongqing, China
Gaura, Elena, Coventry University, UK
Geng, Yanfeng, China University of Petroleum, China
Gole, James, Georgia Institute of Technology, USA
Gong, Hao, National University of Singapore, Singapore
Gonzalez de la Rosa, Juan Jose, University of Cadiz, Spain
Granel, Annette, Goteborg University, Sweden
Graff, Mason, The University of Texas at Arlington, USA
Guan, Shan, Eastman Kodak, USA
Guillet, Bruno, University of Caen, France
Guo, Zhen, New Jersey Institute of Technology, USA
Gupta, Narendra Kumar, Napier University, UK
Hadjiloucas, Sillas, The University of Reading, UK
Haider, Mohammad R., Sonoma State University, USA
Hashsham, Syed, Michigan State University, USA
Hasni, Abdelhafid, Bechar University, Algeria
Hernandez, Alvaro, University of Alcala, Spain
Hernandez, Wilmar, Universidad Politecnica de Madrid, Spain
Homentcovschi, Dorel, SUNY Binghamton, USA
Horstman, Tom, U.S. Automation Group, LLC, USA
Hsiai, Tzung (John), University of Southern California, USA
Huang, Jeng-Sheng, Chung Yuan Christian University, Taiwan
Huang, Star, National Tsing Hua University, Taiwan
Huang, Wei, PSG Design Center, USA
Hui, David, University of New Orleans, USA
Jaffrezic-Renault, Nicole, Ecole Centrale de Lyon, France
James, Daniel, Griffith University, Australia
Janting, Jakob, DELTA Danish Electronics, Denmark
Jiang, Liudi, University of Southampton, UK
Jiang, Wei, University of Virginia, USA
Jiao, Zheng, Shanghai University, China
John, Joachim, IMEC, Belgium
Kalach, Andrew, Voronezh Institute of Ministry of Interior, Russia
Kang, Moonho, Sunmoon University, Korea South
Kaniusas, Eugenijus, Vienna University of Technology, Austria
Katake, Anup, Texas A&M University, USA
Kausel, Wilfried, University of Music, Vienna, Austria
Kavasoglu, Nese, Mugla University, Turkey
Ke, Cathy, Tyndall National Institute, Ireland
Khelfaoui, Rachid, Université de Bechar, Algeria
Khan, Asif, Aligarh Muslim University, Aligarh, India
Kim, Min Young, Kyungpook National University, Korea South
Ko, Sang Choon, Electronics. and Telecom. Research Inst., Korea South
Kotulska, Malgorzata, Wroclaw University of Technology, Poland
Kockar, Hakan, Balikesir University, Turkey
Kong, Ing, RMIT University, Australia
Kratz, Henrik, Uppsala University, Sweden

Krishnamoorthy, Ganesh, University of Texas at Austin, USA
Kumar, Arun, University of Delaware, Newark, USA
Kumar, Subodh, National Physical Laboratory, India
Kung, Chih-Hsien, Chang-Jung Christian University, Taiwan
Lacnjevac, Caslav, University of Belgrade, Serbia
Lay-Ekuakille, Aime, University of Lecce, Italy
Lee, Jang Myung, Pusan National University, Korea South
Lee, Jun Su, Amkor Technology, Inc. South Korea
Lei, Hua, National Starch and Chemical Company, USA
Li, Fengyuan (Thomas), Purdue University, USA
Li, Genxi, Nanjing University, China
Li, Hui, Shanghai Jiaotong University, China
Li, Sihua, Agiltron, Inc., USA
Li, Xian-Fang, Central South University, China
Li, Yuefa, Wayne State University, USA
Liang, Yuanchang, University of Washington, USA
Liawruangrath, Saisunee, Chiang Mai University, Thailand
Liew, Kim Meow, City University of Hong Kong, Hong Kong
Lin, Hermann, National Kaohsiung University, Taiwan
Lin, Paul, Cleveland State University, USA
Linderholm, Pontus, EPFL - Microsystems Laboratory, Switzerland
Liu, Aihua, University of Oklahoma, USA
Liu Changgeng, Louisiana State University, USA
Liu, Cheng-Hsien, National Tsing Hua University, Taiwan
Liu, Songqin, Southeast University, China
Lodeiro, Carlos, University of Vigo, Spain
Lorenzo, Maria Encarnacio, Universidad Autonoma de Madrid, Spain
Lukaszewicz, Jerzy Pawel, Nicholas Copernicus University, Poland
Ma, Zhanfang, Northeast Normal University, China
Majstorovic, Vidosav, University of Belgrade, Serbia
Malyshev, V.V., National Research Centre ‘Kurchatov Institute’, Russia
Marquez, Alfredo, Centro de Investigacion en Materiales Avanzados, Mexico
Matay, Ladislav, Slovak Academy of Sciences, Slovakia
Mathur, Prafull, National Physical Laboratory, India
Maurya, D.K., Institute of Materials Research and Engineering, Singapore
Mekid, Samir, University of Manchester, UK
Melnyk, Ivan, Photon Control Inc., Canada
Mendes, Paulo, University of Minho, Portugal
Mennell, Julie, Northumbria University, UK
Mi, Bin, Boston Scientific Corporation, USA
Minas, Graca, University of Minho, Portugal
Mishra, Vivekanand, National Institute of Technology, India
Moghavvemi, Mahmoud, University of Malaya, Malaysia
Mohammadi, Mohammad-Reza, University of Cambridge, UK
Molina Flores, Esteban, Benemérita Universidad Autónoma de Puebla, Mexico
Moradi, Majid, University of Kerman, Iran
Morello, Rosario, University "Mediterranea" of Reggio Calabria, Italy
Mounir, Ben Ali, University of Sousse, Tunisia
Mrad, Nezih, Defence R&D, Canada
Mulla, Imtiaz Sirajuddin, National Chemical Laboratory, Pune, India
Nabok, Aleksey, Sheffield Hallam University, UK
Neelamegam, Periasamy, Sastra Deemed University, India
Neshkova, Milka, Bulgarian Academy of Sciences, Bulgaria
Oberhammer, Joachim, Royal Institute of Technology, Sweden
Ould Lahoucine, Cherif, University of Guelma, Algeria
Pamidighanta, Sayanu, Bharat Electronics Limited (BEL), India
Pan, Jisheng, Institute of Materials Research & Engineering, Singapore
Park, Joon-Shik, Korea Electronics Technology Institute, Korea South
Passaro, Vittorio M. N., Politecnico di Bari, Italy
Penza, Michele, ENEA C.R., Italy
Pereira, Jose Miguel, Instituto Politecnico de Setebal, Portugal
Petsev, Dimiter, University of New Mexico, USA
Pogacnik, Lea, University of Ljubljana, Slovenia
Post, Michael, National Research Council, Canada
Prance, Robert, University of Sussex, UK
Prasad, Ambika, Gulbarga University, India
Prateepasen, Asa, Kingmoungut's University of Technology, Thailand
Pugno, Nicola M., Politecnico di Torino, Italy
Pullini, Daniele, Centro Ricerche FIAT, Italy
Pumera, Martin, National Institute for Materials Science, Japan
Radhakrishnan, S. National Chemical Laboratory, Pune, India
Rajanna, K., Indian Institute of Science, India
Ramadan, Qasem, Institute of Microelectronics, Singapore
Rao, Basuthkar, Tata Inst. of Fundamental Research, India
Raoof, Kosai, Joseph Fourier University of Grenoble, France
Rastogi Shiva, K. University of Idaho, USA
Reig, Candid, University of Valencia, Spain
Restivo, Maria Teresa, University of Porto, Portugal
Robert, Michel, University Henri Poincare, France
Rezazadeh, Ghader, Urmia University, Iran
Royo, Santiago, Universitat Politecnica de Catalunya, Spain
Rodriguez, Angel, Universidad Politecnica de Cataluna, Spain
Rothberg, Steve, Loughborough University, UK
Sadana, Ajit, University of Mississippi, USA
Sadeghian Marnani, Hamed, TU Delft, The Netherlands
Sapozhnikova, Ksenia, D.I.Mendeleyev Institute for Metrology, Russia
Sandacci, Serghei, Sensor Technology Ltd., UK
Saxena, Vibha, Bhbha Atomic Research Centre, Mumbai, India
Schneider, John K., Ultra-Scan Corporation, USA
Sengupta, Deepak, Advance Bio-Photonics, India
Seif, Selemani, Alabama A & M University, USA
Seifter, Achim, Los Alamos National Laboratory, USA
Shah, Kriyang, La Trobe University, Australia
Sankarraj, Anand, Detector Electronics Corp., USA
Silva Girao, Pedro, Technical University of Lisbon, Portugal
Singh, V. R., National Physical Laboratory, India
Slomovitz, Daniel, UTE, Uruguay
Smith, Martin, Open University, UK
Soleimanpour, Amir Masoud, University of Toledo, USA
Soleymanpour, Ahmad, University of Toledo, USA
Somani, Prakash R., Centre for Materials for Electronics Technol., India
Sridharan, M., Sastra University, India
Srinivas, Talabattula, Indian Institute of Science, Bangalore, India
Srivastava, Arvind K., NanoSonix Inc., USA
Stefan-van Staden, Raluca-Ioana, University of Pretoria, South Africa
Stefanescu, Dan Mihai, Romanian Measurement Society, Romania
Sumriddetchka, Sarun, National Electronics and Comp. Technol. Center, Thailand
Sun, Chengliang, Polytechnic University, Hong-Kong
Sun, Dongming, Jilin University, China
Sun, Junhua, Beijing University of Aeronautics and Astronautics, China
Sun, Zhiqiang, Central South University, China
Suri, C. Raman, Institute of Microbial Technology, India
Sysoev, Victor, Saratov State Technical University, Russia
Szewczyk, Roman, Industr. Research Inst. for Automation and Measurement, Poland
Tan, Ooi Kiang, Nanyang Technological University, Singapore,
Tang, Dianping, Southwest University, China
Tang, Jaw-Luen, National Chung Cheng University, Taiwan
Teker, Kasif, Frostburg State University, USA
Thirunavukkarasu, I., Manipal University Karnataka, India
Thumbavanam Pad, Kartik, Carnegie Mellon University, USA
Tian, Gui Yun, University of Newcastle, UK
Tsiantos, Vassilios, Technological Educational Institute of Kaval, Greece
Tsigara, Anna, National Hellenic Research Foundation, Greece
Twomey, Karen, University College Cork, Ireland
Valente, Antonio, University, Vila Real, - U.T.A.D., Portugal
Vanga, Raghav Rao, Summit Technology Services, Inc., USA
Vaseashta, Ashok, Marshall University, USA
Vazquez, Carmen, Carlos III University in Madrid, Spain
Vieira, Manuela, Instituto Superior de Engenharia de Lisboa, Portugal
Vigna, Benedetto, STMicroelectronics, Italy
Vrba, Radimir, Brno University of Technology, Czech Republic
Wandelt, Barbara, Technical University of Lodz, Poland
Wang, Jiangping, Xi'an Shiyou University, China
Wang, Kedong, Beihang University, China
Wang, Liang, Pacific Northwest National Laboratory, USA
Wang, Mi, University of Leeds, UK
Wang, Shinn-Fwu, Ching Yun University, Taiwan
Wang, Wei-Chih, University of Washington, USA
Wang, Wensheng, University of Pennsylvania, USA
Watson, Steven, Center for NanoSpace Technologies Inc., USA
Weiping, Yan, Dalian University of Technology, China
Wells, Stephen, Southern Company Services, USA
Wolkenberg, Andrzej, Institute of Electron Technology, Poland
Woods, R. Clive, Louisiana State University, USA
Wu, DerHo, National Pingtung Univ. of Science and Technology, Taiwan
Wu, Zhaoyang, Hunan University, China
Xiu Tao, Ge, Chuzhou University, China
Xu, Lisheng, The Chinese University of Hong Kong, Hong Kong
Xu, Sen, Drexel University, USA
Xu, Tao, University of California, Irvine, USA
Yang, Dongfang, National Research Council, Canada
Yang, Shuang-Hua, Loughborough University, UK
Yang, Wuqiang, The University of Manchester, UK
Yang, Xiaoling, University of Georgia, Athens, GA, USA
Yaping Dan, Harvard University, USA
Ymeti, Aurel, University of Twente, Netherland
Yong Zhao, Northeastern University, China
Yu, Haihu, Wuhan University of Technology, China
Yuan, Yong, Massey University, New Zealand
Yufera Garcia, Alberto, Seville University, Spain
Zakaria, Zulkarnay, University Malaysia Perlis, Malaysia
Zagnoni, Michele, University of Southampton, UK
Zamani, Cyrus, Universitat de Barcelona, Spain
Zeni, Luigi, Second University of Naples, Italy
Zhang, Minglong, Shanghai University, China
Zhang, Qintao, University of California at Berkeley, USA
Zhang, Weiping, Shanghai Jiao Tong University, China
Zhang, Wenming, Shanghai Jiao Tong University, China
Zhang, Xueji, World Precision Instruments, Inc., USA
Zhong, Haoxiang, Henan Normal University, China
Zhu, Qing, Fujifilm Dimatix, Inc., USA
Zorzano, Luis, Universidad de La Rioja, Spain
Zourob, Mohammed, University of Cambridge, UK

Sensors & Transducers Journal (ISSN 1726-5479) is a peer review international journal published monthly online by International Frequency Sensor Association (IFSA).
Available in electronic and on CD. Copyright © 2012 by International Frequency Sensor Association. All rights reserved.

Sensors & Transducers Journal

Contents

Volume 15
Special Issue
October 2012

www.sensorsportal.com

ISSN 1726-5479

Research Articles

Shock Resistance of MEMS Capacitive Accelerometers
Yongkang Tao, Yunfeng Liu, and Jingxin Dong 1

Research on Nonlinear Vibration in Micro-machined Resonant Accelerometer
Shuming Zhao, Yunfeng Liu, Fan Wang, Jingxin Dong 14

Reversible and Irreversible Temperature-induced Changes in Exchange-biased Planar Hall Effect Bridge (PHEB) Magnetic Field Sensors
G. Rizzi, N. C. Lundtoft, F. W. Østerberg, M. F. Hansen 22

Synthesis and Characterization of Nickel Ferrite ($NiFe_2O_4$) Nanoparticles with Silver Addition for H_2S Gas Detection
N. Domínguez-Ruiz, P. E. García-Casilla, J. F. Hernández-Paz, R. C. Ambrosio-Lázaro, M. Ramos-Murillo, H. Camacho-Montes, C. A. Rodríguez González 35

Electron-Relay Supercapacitor Mimics Electrophorus Electricus's Reversible Membrane Potential for a High Rate Discharge Pulse
Ellen T. Chen and Christelle Ngatchou 42

Ultralow Detection of Bio-markers Using Gold Nanoshells
Dhruvinkumar Patel, Xinghua Sun, Guandong Zhang, Robert S. Keynton, Andre M. Gobin 49

Evaluation of Anchoring Materials for Ultra-Sensitive Biosensors Modified with Au Nanoparticles and Enzymes
Solomon W. Leung, David Assan and James C. K. Lai 59

Authors are encouraged to submit article in MS Word (doc) and Acrobat (pdf) formats by e-mail: editor@sensorsportal.com
Please visit journal's webpage with preparation instructions: http://www.sensorsportal.com/HTML/DIGEST/Submition.htm

International Frequency Sensor Association (IFSA).

International Frequency Sensor Association Publishing

Call for Books Proposals

Sensors, MEMS, Measuring instrumentation, etc.

Benefits and rewards of being an IFSA author:

1 Royalties

Today IFSA offers most high royalty in the world: you will receive 50 % of each book sold in comparison with 8-11 % from other publishers, and get payment on monthly basis compared with other publishers' yearly basis.

2 Quick Publication

IFSA recognizes the value to our customers of timely information, so we produce your book quickly: 2 months publishing schedule compared with other publishers' 5-18-month schedule.

3 The Best Targeted Marketing and Promotion

As a leading online publisher in sensors related fields, IFSA and its Sensors Web Portal has a great expertise and experience to market and promote your book worldwide. An extensive marketing plan will be developed for each new book, including intensive promotions in IFSA's media: journal, magazine, newsletter and online bookstore at Sensors Web Portal.

4 Published Format: printable pdf (Acrobat).

When you publish with IFSA your book will never go out of print and can be delivered to customers in a few minutes.

You are invited kindly to share in the benefits of being an IFSA author and to submit your book proposal or/and a sample chapter for review by e-mail to **editor@sensorsportal.com** These proposals may include technical references, application engineering handbooks, monographs, guides and textbooks. Also edited survey books, state-of-the art or state-of-the-technology, are of interest to us. For more detail please visit: **http://www.sensorsportal.com/HTML/IFSA_Publishing.htm**

International Frequency Sensor Association (IFSA) Publishing

NEW BOOK

Jacob Y. Wong, Roy L. Anderson

Non-Dispersive Infrared Gas Measurement

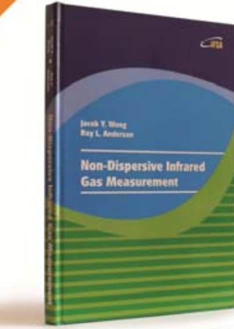

Formats: printable pdf (Acrobat) and print (hardcover),120 pages

ISBN: 978-84-615-9732-1,
e-ISBN: 978-84-615-9512-9

Written by experts in the field, the *Non-Dispersive Infrared Gas Measurement* begins with a brief survey of various gas measurement techniques and continues with fundamental aspects and cutting-edge progress in NDIR gas sensors in their historical development.

- It addresses various fields, including:
- Interactive and non-interactive gas sensors
- Non-dispersive infrared gas sensors' components
- Single- and Double beam designs
- Historical background and today's of NDIR gas measurements

Providing sufficient background information and details, the book Non-Dispersive Infrared Gas Measurement is an excellent resource for advanced level undergraduate and graduate students as well as researchers, instrumentation engineers, applied physicists, chemists, material scientists in gas, chemical, biological, and medical sensors to have a comprehensive understanding of the development of non-dispersive infrared gas sensors and the trends for the future investigation.

http://sensorsportal.com/HTML/BOOKSTORE/NDIR_Gas_Measurement.htm

Sensors & Transducers Journal, Vol. 15, Special Issue, October 2012, pp. 22-34

Sensors & Transducers

ISSN 1726-5479
© 2012 by IFSA
http://www.sensorsportal.com

Reversible and Irreversible Temperature-induced Changes in Exchange-biased Planar Hall Effect Bridge (PHEB) Magnetic Field Sensors

G. Rizzi, N. C. Lundtoft, F. W. Østerberg, * M. F. Hansen
Department of Micro- and Nanotechnology, Technical University of Denmark
DTU Nanotech, Building 345B, DK-2800 Kongens Lyngby, Denmark
* E-mail: Mikkel.Hansen@nanotech.dtu.dk

Received: 14 September 2012 /Accepted: 1 October 2012 /Published: 8 October 2012

Abstract: We investigate the changes of planar Hall effect bridge magnetic field sensors prepared without field annealing and with field annealing at 240 °C, 280 °C and 320 °C when these are exposed to temperatures between 25 °C and 90 °C. From analyses of the sensor response vs. magnetic field we extract the exchange bias field H_{ex}, the uniaxial anisotropy field H_K and the anisotropic magnetoresistance (AMR) of the exchange biased thin films at a given temperature. By comparing measurements carried out at elevated temperatures T with measurements carried out at 25 °C after exposure to T, we separate the reversible from the irreversible changes of the sensors. The un-annealed sample shows a significant irreversible change of H_{ex} and H_K upon exposure to temperatures above room temperature. The irreversible changes are significantly reduced but not eliminated by the low-temperature field annealing. The reversible changes with temperature are essentially the same for all samples. The results are not only relevant for sensor applications but also demonstrate the method as a useful tool for characterizing exchange-biased thin films. *Copyright © 2012 IFSA.*

Keywords: Magnetic biosensors, Planar Hall effect, Exchange bias, Anisotropic magnetoresistance.

1. Introduction

For applications of any sensor, it is important to know and correct for the effect of varying temperatures of the sensor environment. Moreover, it is important to be aware of irreversible changes of the sensor parameters induced by varying temperatures of the environment. Planar Hall effect magnetic field sensors have proven attractive for magnetic field sensing due to their low intrinsic noise

and potentially high signal-to-noise ratio [1]. We are investigating exchange-biased planar Hall effect sensors for magnetic biodetection [2, 3].

Here, we systematically study the changes of the response of planar Hall effect bridge sensors [4] upon exposure of these to temperatures between 25 °C and 90 °C. These temperatures correspond to the range typically employed in DNA based assays with amplification by polymerase chain reaction (PCR). From analyses of magnetic field sweeps of the sensor response we extract the parameters of thin film sensor stacks at all investigated temperatures and by performing measurements at 25 °C performed after all measurements at elevated temperatures we quantify and distinguish reversible and irreversible changes of each of the sensor parameters. These studies are carried out for a stack which is not exposed to any magnetic field annealing and for stacks that are field annealed at 240 °C, 280 °C and 320 °C. The results are generally relevant for applications of exchange-biased thin film sensors and demonstrate the method as a general tool for studying thin film magnetic properties vs. temperature.

2. Sensor Model

Below, we consider a material showing anisotropic magnetoresistance (AMR) with resistivities $\rho_{\parallel}$ and $\rho_{\perp}$ parallel and perpendicular to the magnetization vector **M**, respectively. The AMR ratio, defined as $\Delta\rho/\rho_{av}$, where $\Delta\rho \equiv \rho_{\parallel}-\rho_{\perp}$ and $\rho_{av} \equiv \rho_{\parallel}/3+2\rho_{\perp}/3$, assumes a value of 2-3 % for permalloy ($Ni_{80}Fe_{20}$). Fig. 1 shows a Wheatstone bridge consisting of four pairwise identical elements of the material of width w and length l. The resistance of a single element forming an angle α to the x-axis and with a homogeneous magnetization forming an angle θ to the x-axis is [4]

$$R(\alpha,\theta) = \tfrac{l}{wt}\left[\tfrac{1}{2}\left(\rho_{\parallel} + \rho_{\perp}\right) - \tfrac{1}{2}\Delta\rho\cos\left[2(\theta-\alpha)\right]\right], \tag{1}$$

where t is the thickness of the element. A current I injected in the x-direction results in the bridge output

$$V_y = \tfrac{1}{2} I\left[R(\alpha_+,\theta_+) - R(\alpha_-,\theta_-)\right], \tag{2}$$

where the orientation of magnetization of the elements forming angles α_+ and α_- to the x-axis are denoted θ_+ and θ_-. The maximum bridge output, obtained when $\alpha_+ = -\alpha_- = \pi/4$, is given by

$$V_y = \tfrac{1}{4} I\,\Delta\rho\,\tfrac{l}{wt}\left[\sin(2\theta_+) + \sin(2\theta_-)\right] \equiv \tfrac{1}{4} V_{pp}\left[\sin(2\theta_+) + \sin(2\theta_-)\right], \tag{3}$$

where we have introduced the nominal peak-to-peak sensor output voltage $V_{pp} = I\Delta\rho l/(wt)$ [4]. Equation (3) is identical to the output voltage from a cross-geometry planar Hall effect sensor multiplied by the geometrical amplification factor l/w. Therefore, we have termed the above sensors planar Hall effect bridge (PHEB) sensors [4].

Theoretically, the angles θ_+ and θ_- can be found by minimizing the single domain energy density for α_+ and α_-, respectively. We divide the volume energy density by the saturation flux density to form the normalized energy density u

$$u = -H_y\sin\theta - H_{ex}\cos\theta - \tfrac{1}{2}H_K\cos^2\theta - \tfrac{1}{2}H_s\cos^2(\alpha-\theta), \tag{4}$$

which expresses the energy density in units of the H-field. In Eq. (4), H_y is the external magnetic field applied in the y-direction, H_{ex} is the exchange field due to a unidirectional anisotropy along $\theta = 0$,

H_K is the anisotropy field due to a uniaxial anisotropy along $\theta = 0$ and H_s is the shape anisotropy field of the element (preferring a magnetization orientation with $\theta = \alpha$). Defining the demagnetization factors along and perpendicular to an element as $N_{\|}$ and $N_{\perp}$, respectively, the shape anisotropy field is $H_s = (N_{\perp} - N_{\|})M_s$ [5]. Our previous work [4] considered only the case of negligible shape anisotropy where $\theta_+ = \theta_- = \theta$.

We write the low-field sensor output voltage as

$$V_y = S_0 I H_y, \quad (5)$$

where we have defined the low-field sensitivity S_0. For negligible shape anisotropy, minimization of Eq. (4) for $H_s = 0$ and small values of θ yields

$$S_0 = \frac{l}{w}\frac{\Delta\rho}{t}\frac{1}{H_K + H_{ex}}. \quad (6)$$

If the shape anisotropy is significant but still small, the sensor response curve will be modified such that it flattens near zero applied field, resulting in a decrease of S_0 compared to Eq. (6), while still maintaining a peak-to-peak signal V_{pp} given by Eq. (3) (unpublished results).

3. Experimental

A batch of four wafers with top-pinned PHEB sensors was prepared on 4” silicon substrates with a 1 μm thick thermally grown oxide as follows: First, the stack Ta(3 nm)/$Ni_{80}Fe_{20}$(30 nm)/$Mn_{80}Ir_{20}$ (20 nm)/Ta(3 nm) was grown in a K. J. Lesker company CMS 18 multitarget sputter system in an Argon pressure of 3 mTorr with an RF substrate bias of 3W. The easy magnetization direction and axis of the permalloy layer were defined by applying a uniform magnetic field of $\mu_0 H_x = 20$ mT along the x-axis during the deposition. Subsequently, contacts of Ti(10 nm)/Pt(100 nm)/Au(100 nm)/Ti(10 nm) were deposited by e-beam evaporation and defined by lift-off. The negative lithography process employed a reversal baking step at 120 °C for 120 s on a hot plate in zero magnetic field.

One of the nominally identical four wafers was not given any further treatment and was labeled ‘not annealed’/’un-annealed’. The other three wafers were annealed in vacuum in the sputter deposition chamber at temperatures of 240 °C, 280 °C and 320 °C for 1 hour in the presence of a saturating magnetic field $\mu_0 H_x = 20$ mT applied along the x-axis.

The dimensions of the elements of all investigated sensors were w=20 μm and l = 280 μm (Fig. 1). All sensors were surrounded by magnetic stack with a 3 μm gap to reduce the shape anisotropy of the elements. The simple theory presented in section 2 accounts for the elements but not the corners connecting the elements. The effect of corners was therefore investigated by finite element analysis of the sensor output for a single domain sensor structure. The calculations showed a sensor response that can be described by an effective sensor aspect ratio l/w = 14.87, which is 6% higher than the nominal one of l/w=14.

The magnetic properties of continuous thin films with dimensions 3×3 mm^2 were characterized for all four wafers using a LakeShore model 7407 vibrating sample magnetometer (VSM) and values of H_{ex} and H_K were extracted from easy axis hysteresis loop measurements.

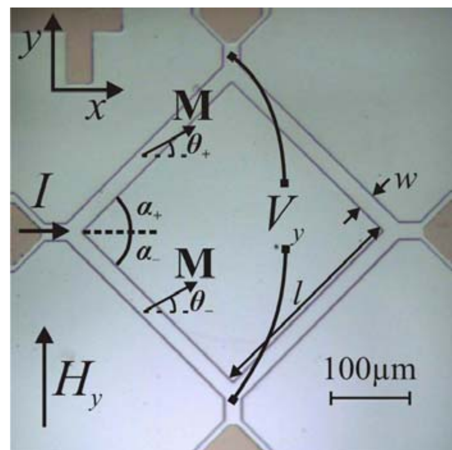

Fig. 1. Image of planar Hall effect magnetic bridge sensor with definition of geometric variables and symbols.

Values of the stack sheet resistances $\rho_{\|}/t$ and $\rho_{\perp}/t$ for the four wafers were obtained from electrical measurements of the resistance on transmission line test structures placed near the investigated sensor chips on the wafers in saturating magnetic fields applied parallel and perpendicular to the current, respectively.

Measurements of the sensor response vs. applied field were carried out as follows: the sensors were biased with an alternating current of root-mean-square (RMS) amplitude I_{RMS} = 1/√2 mA and frequency f = 65 Hz provided by a Keithley 6221 precision current source. A Stanford Research Systems model SR830 lock-in amplifier was used to record the first harmonic in-phase root-mean-square (RMS) signal $V_{y,\mathrm{RMS}}$. Note, that Eq. (3) also holds for the RMS values I_{RMS} and $V_{y,\mathrm{RMS}}$. To simplify the notation below, we will therefore refer to the RMS values as V_y and I. The applied magnetic field $\mu_0 H_y$ was generated by a custom built electromagnet and monitored using commercially available Hall probes. Field sweeps were carried out by sweeping the field in both directions between $\mu_0 H_y = \pm 40$ mT. The sensor temperature was regulated to stability better than 0.1°C by use of a Peltier element, platinum RTD and a precision temperature controller. Sensor characteristics of all sensors were measured at temperatures from 25°C to 90°C in steps of 10°C. Each measurement performed at an elevated temperature was followed by a reference measurement performed at 25°C.

In addition, we also studied the effect of repeated exposure to 90 °C for an un-annealed sensor and a sensor from the wafer that was field annealed at 280 °C. These temperature cycling experiments were carried out as follows: first, the temperature was set to 25 °C and left for 10 min before a field sweep was carried out. The field sweep took about 8 min to complete. Then, the temperature was set to 90 °C and the measurement procedure was repeated. Finally, this cycle between 25 °C and 90 °C was repeated for about 7 hours.

4. Results

4.1. As Deposited Samples

In this section, we present results obtained for the samples at 25 ºC in their as-deposited state (i.e. prior to sensor characterization at elevated temperatures). We establish the model used for analyzing the field sweeps and compare to electrical and magnetic reference measurements.

The sensor signal V_y normalized with the bias current I, was measured vs. the sweeping field H_y for all four wafers. Fig. 2 shows the initial field sweeps measured for the samples with no annealing and with annealing at 280 °C. The annealing is observed to shift the peak of the sensor response towards lower field values and to increase the low-field sensitivity. The peak-to-peak value of the sensor response is found to be essentially unchanged by the annealing.

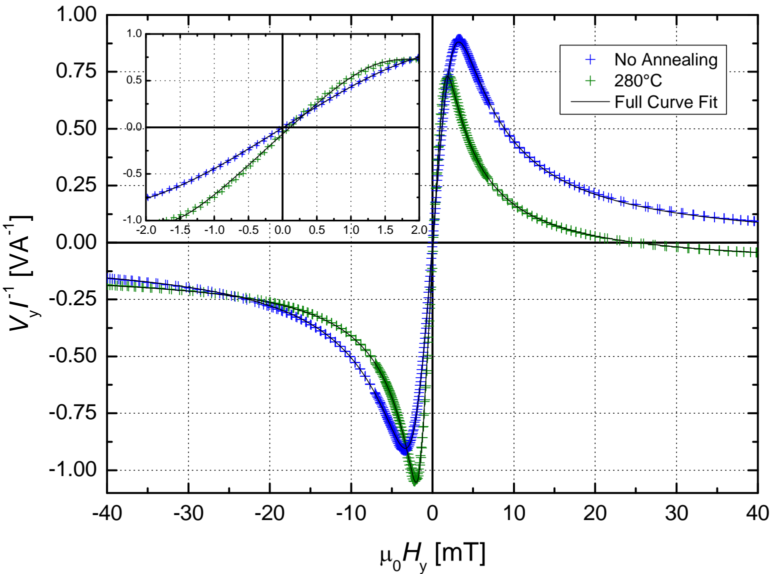

Fig. 2. Normalized sensor output (V_y/I) vs. external field (H_y) for sensors from the wafers with no annealing and with field annealing at 280°C in their initial condition. The inset shows the low-field region of the sensor response. The lines are fits to the single domain model for the sensor response described in the text.

The solid lines in Fig. 2 are least-squares fits to Eq. (3) with values of θ_+ and θ_- obtained by minimizing Eq. (4). The investigated free parameters in the fitting were V_{pp}/I , H_{ex} and H_K. The value of H_s was found to vary only marginally between the different temperature and annealing conditions and was fixed to the average value $\mu_0 H_s$ = 0.789 mT obtained from fitting data for all sensors and temperatures with this parameter set free. In the fitting we also allowed for offsets in the sensor output and the applied field. The quality of all fits was comparable to those shown in Fig. 2. Table 1 shows the values of $\mu_0 H_{ex}$ and $\mu_0 H_K$ obtained from the VSM measurements, the values of $\Delta\rho/t$ and the AMR ratio obtained from reference electrical measurements on the transmission line structure as well as the values of $\mu_0 H_{ex}$, $\mu_0 H_K$, S_0 and V_{pp}/I obtained from fits to field sweeps of the sensor response. Values reported for the low-field sensitivities S_0 were taken as the slope of the fits between ±0.15 mT.

Table 1. Parameters of the magnetic stack obtained from VSM measurements, electrical measurements on a transmission line structure and from fits to sensor field sweeps. All measurements were carried out at 25ºC on as-deposited samples (i.e. prior to any experiments at elevated temperatures). Numbers in parentheses indicate the uncertainties reported by the least squares fitting routine.

Annealing conditions	VSM		Electrical ref.		Sensor field sweeps			
	$\mu_0 H_{ex}$ [mT]	$\mu_0 H_K$ [mT]	$\Delta\rho/t$ [Ω]	AMR [%]	$\mu_0 H_{ex}$ [mT]	$\mu_0 H_K$ [mT]	S_0 [V/(AT)]	V_{pp}/I [V/A]
No annealing	2.89(5)	0.39(5)	0.1296(1)	1.88	2.66(1)	0.90(3)	465	1.779(2)
240 °C	2.02(5)	0.41(5)	0.1318(1)	2.03	1.91(1)	0.52(2)	637	1.785(3)
280 °C	1.90(5)	0.50(5)	0.1319(3)	1.95	1.60(1)	0.50(2)	699	1.764(4)
320 °C	1.39(5)	0.46(5)	0.1317(1)	2.03	1.32(1)	0.34(3)	807	1.768(7)

The values of H_{ex} obtained from VSM measurements and fits to the sensor field sweeps correspond well to each other although the values from the field sweeps are slightly lower than those obtained from the VSM measurements. The values of H_K obtained by VSM and from the sensor field sweeps are comparable for the annealed samples, but they differ about a factor of two for the un-annealed sample. The main effect of the low-temperature annealing is that H_{ex} is found to decrease monotonously with increasing annealing temperature. A decrease of about a factor of two is observed for annealing at 320 °C. The values of H_K extracted from the sensor field sweeps are found to decrease with increased annealing temperature, whereas no systematic change is found from the VSM studies. The value of $\Delta\rho/t$ remains essentially unchanged by the annealing. The low-field sensitivity is found to increase with annealing and increases almost by a factor of two for the highest annealing temperature.

4.2. Temperature Dependence of Parameters

In this section, we first present results of the experiments carried out at elevated temperatures for the un-annealed sample and show that our measurement procedure enables us to clearly distinguish reversible and irreversible changes of the sensor parameters upon exposure to a given elevated temperature. Then, we report the results of the corresponding experiments carried out on sensors from the low-temperature field annealed wafers. All parameters shown below have been obtained from fits to sensor field sweeps as described in section 4.1.

Fig. 3 shows the values of S_0, H_{ex} and H_K obtained from analysis of sensor field sweeps in a series of experiments carried out on a sensor from the wafer with no annealing at sequentially increasing temperatures T. First, the sensor response was measured at 25 °C. Then, the temperature was increased to 30 °C and the sensor response was measured after a waiting time of 2 min and finally, the temperature was reduced to 25 °C to carry out a reference measurement after a waiting time of 2 min. This procedure was repeated for temperatures increasing up to 90 °C in steps of 10 °C. The sensor parameters measured at the elevated temperature T result from the sum of reversible and irreversible changes, whereas the series of reference measurements carried out at 25 °C show only the irreversible changes. This enables us to clearly distinguish the reversible and irreversible changes of the sensor parameters as indicated by the colored areas in Fig. 3.

In Fig. 3, the value of S_0 is found to increase about 20% when the temperature is increased from 25 °C to 90 °C. Slightly more than half of this increase is irreversible. The values of H_{ex} and H_K are found to decrease approximately linearly with increasing temperature with temperature coefficients of −0.42%/°C (27% total decrease) and −0.68%/°C (44% total decrease), respectively, in good agreement with a previous study [6]. For H_{ex} about 20% of the change is irreversible and for H_K about 50 % of the change is irreversible. Thus, the irreversible changes are significant for this sample.

Corresponding series of experiments were carried out for the wafers exposed to the low-temperature field annealing.

Fig. 4(a) shows the values of V_{pp}/I for the measurements carried out on all samples. These values are proportional to $\Delta\rho/t$. The values obtained at 25 °C are close to identical and show no systematic variation with annealing conditions. Upon exposure to elevated temperatures, the values are found to decrease linearly with temperature with a temperature coefficient of −0.22 %/°C. The change is found to be fully reversible, i.e. no irreversible changes result from the increased temperature. This shows that the low-temperature field annealing and the experiments performed at elevated temperatures do not result in any detectable changes of the AMR properties of the sensor stack.

Fig. 4(b) shows the values of the low-field sensitivities S_0 normalized to the initial values obtained at 25 °C (given in Table 1) for the four investigated wafers as function of the measuring temperature T.

The data for the sample with no field annealing from Fig. 3 are shown for comparison. The field annealed samples show a much smaller temperature variation than the sample with no annealing. For the sample annealed at 240 °C the relative change of S_0 is about 7 % when the temperature is increased to 80 °C, but more than half of this change is irreversible. For the sample annealed at 280 °C, the points measured at T coincide with the reference points measured at 25 °C, indicating that the entire change of S_0 of about 3 % is irreversible. For the sample annealed at 320 °C, there is a net decrease of S_0 with T of about 2 % resulting from an irreversible increase of S_0 of about 3 % and a reversible decrease of S_0 of about 5 %.

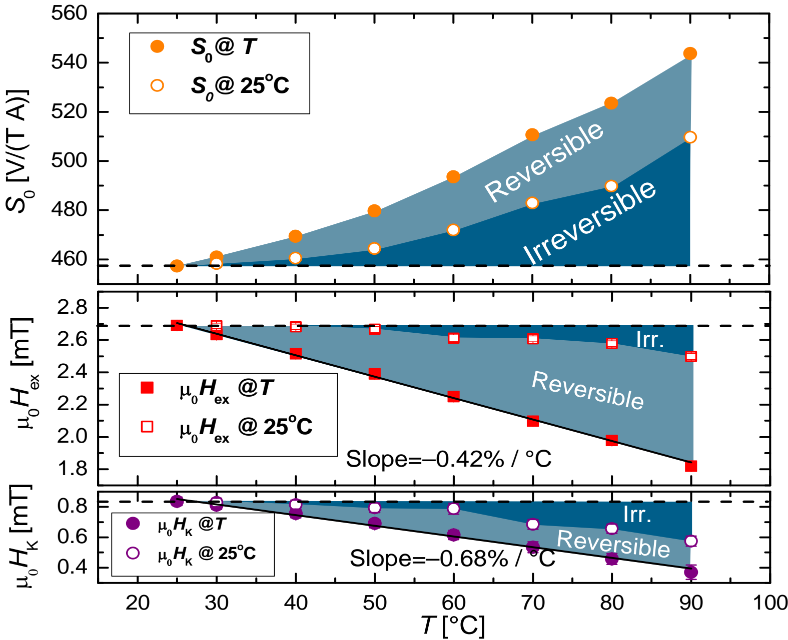

Fig. 3. Values of S_0 (top), H_{ex} (middle) and H_K (bottom) extracted from fits of the field sweeps on the un-annealed sample. Filled points are measured at temperature T, empty points are measured at the reference temperature 25°C after exposure to T. The full lines are linear fits corresponding to the indicated temperature coefficients.

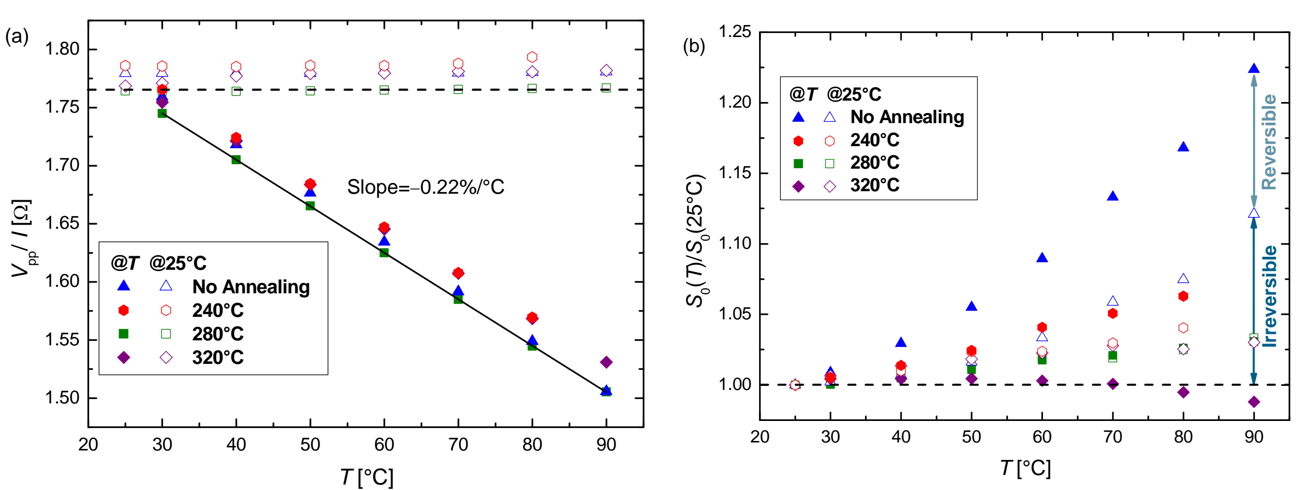

Fig. 4. Values of (a) the peak-to-peak sensor response V_{pp}/I and (b) the low-field sensitivity S_0 normalized to its initial value at 25°C obtained from field sweep fits. Different data sets are for sensors from wafers with the indicated annealing conditions. Filled points are measured at T, open points are measured at 25 °C after exposure to temperature T. The arrows to the right indicate the reversible and irreversible change for the un-annealed sample at T=90 °C.

Figs. 5(a) and (b) show the values of H_{ex} (normalized to their initial values given in Table 1) and H_K obtained for the four investigated wafers as function of the measuring temperature T, respectively. For all annealing conditions, the reversible change of H_{ex} with temperature is linear and can be described by the temperature coefficient –0.37%/°C. For the un-annealed sample the irreversible change of H_{ex} is about 8 % when the temperature is increased from 25 °C to 90 °C. The field annealed samples show a smaller, but not negligible irreversible change of H_{ex}, which appears to be independent of the annealing temperature.

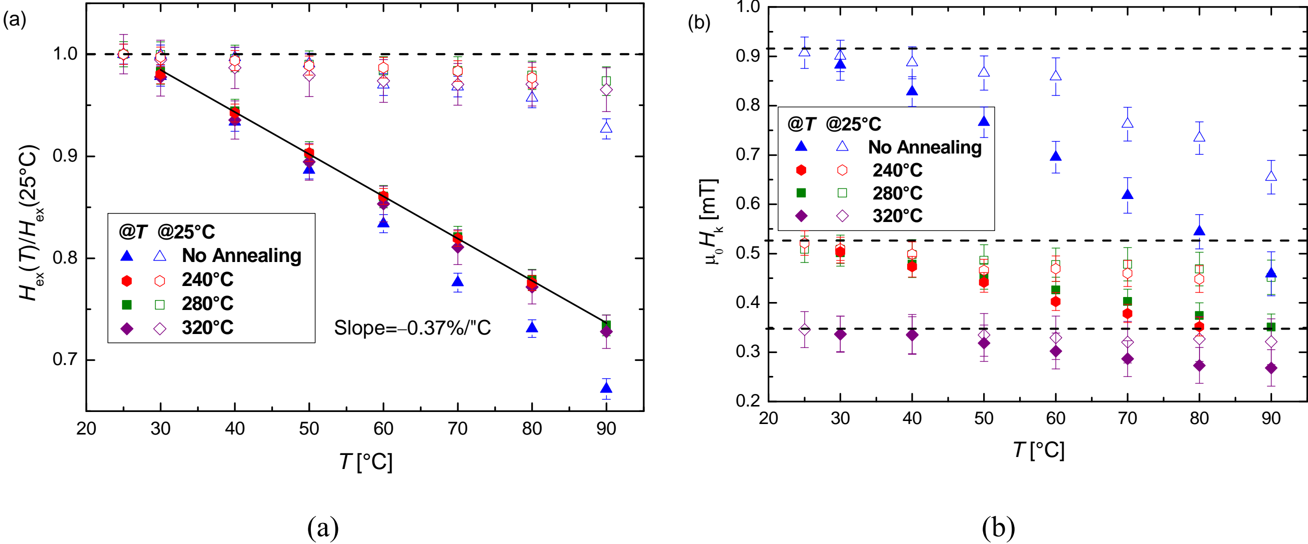

(a) (b)

Fig. 5. Values of (a) the normalized exchange bias field $H_{ex}(T)/H_{ex}(25°C)$ and (b) the anisotropy field H_K. Different data sets are for sensors from wafers with the indicated annealing conditions. Filled points are measured at T, open points are measured at 25 °C after exposure to temperature T. The dashed lines indicate the initial values of the parameters.

The initial values of H_K are found to decrease monotonically with annealing conditions. For the sample with no field annealing, the value of H_K changes almost 50 % when the temperature is increased from 25 °C to 90 °C and approximately half of this change is irreversible. The field annealed samples show a much smaller change and the irreversible change is smaller than the error on the individual points (and smallest for the sample annealed at 320 °C). The reversible decrease of H_K with temperature for these samples is about 20 %.

4.3. Temperature Cycling

Fig. 6 shows the effect of prolonged exposure at 90 °C on S_0, H_{ex} and H_K vs. the time of the temperature cycling experiment. Note, that only half of this time was spent at 90°C. Field sweeps were measured on the sensor annealed at 280 °C and on the un-annealed sensor while cycling the temperature between 25 °C and 90 °C with each temperature step taking 18 min. The lines in Fig. 6 connect points measured at the same temperature. The extracted values for the different parameters are normalized by the value reached at 90 °C after about 7 h of temperature cycling.

Fig. 6(a) shows the normalized value of S_0 vs. the time of the temperature cycling experiment. As for the results discussed above, the sensitivity of the sensor annealed at 280 °C changes little upon heating compared to the un-annealed sensor. The parameters obtained at 25 °C for the un-annealed wafer show a big change (>7 %) after first exposure at 90 °C and then slowly approach their asymptotic values.

For this sample, the sensitivity at 25 °C still changes after 7h of cycling with a total irreversible change of about 20 %. The values measured during the cycle steps at 90 °C show a similar settling over a period of hours. The chip from the wafer annealed at 280 °C shows a significant initial change in the first cycle after which the parameters slowly settle near their asymptotic values. Thus, for this sample, the irreversible change of S_0 is less than 5 % during the whole cycling experiment, and the value at 25 °C reaches 98.4 % of its final value after the first exposure to 90 °C.

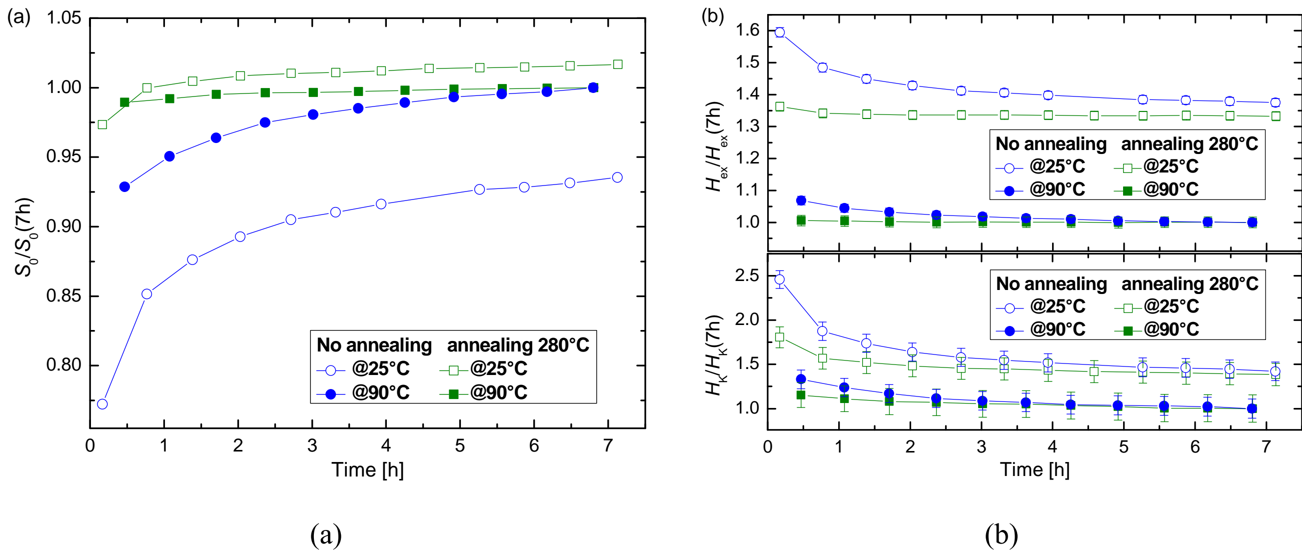

(a) (b)

Fig. 6. Values of (a) low-field sensitivity S_0 and (b) H_{ex} and H_K normalized by their value measured at 90 °C after 7 h temperature cycling between 25 °C and 90 °C. Different data sets are for sensors from wafers with the indicated annealing conditions. Filled points are measured at 90 °C open points are measured at 25 °C. The temperature was cycled between 25 °C and 90 °C, each temperature was held constant for 18 min.

Fig. 6(b) shows the corresponding normalized values of H_{ex} and H_K. The value of H_{ex} measured at 25 °C decreases for both sensors but the relative change for the annealed sensor is seven times smaller than for the un-annealed sensor. Again, the values measured at 90 °C show a similar behavior. The relative change in H_K is bigger than for H_{ex} for both sensors, although the change for the un-annealed sensor is twice as big as that for the sample annealed at 280 °C. We also notice for both H_{ex} and H_K and independent of low-temperature field annealing that the ratio between the values obtained at 90 °C and 25 °C approach the same value.

5. Discussion

5.1. Analysis Method

The presented single domain model for the sensor response provides excellent fits of all measured field sweeps. The parameters obtained from the fits are generally found to agree well with corresponding parameters obtained by VSM and on electrical reference samples although some differences appear. In section 4.1 in Table 1 that the value of H_K from the fits of the sensor measurements was about twice that obtained from the VSM measurements. This difference is in agreement with previous studies [6] and is attributed to effects of the sensor structuring.

Assuming negligible shape anisotropy, the low-field sensitivity is given by $S_0 = (l/w)(\Delta\rho/t)(H_{ex}+H_K)^{-1}$ (cf. Eq. (6)) and the peak-to-peak sensor output is given by $V_{pp}/I = (\Delta\rho/t)(l/w) = 14.87(\Delta\rho/t)$

(cf. Eq. (3)). Inserting the values for the reference samples, we find that the measured low-field sensitivities are generally about 20 % lower than the calculated values and the measured values of V_{pp}/I are about 9 % smaller than the calculated values. This is attributed to demagnetization effects due to the sensor geometry, which cause the magnetization of the sensor elements to deviate from the nominal single domain state near their edges [7]. From fits we found the shape anisotropy field $\mu_0 H_s$ = 0.789 mT, which is comparable to the values of $\mu_0 H_{ex}$ and $\mu_0 H_K$ reported in Table 1 and hence is significant.

These results indicate that the even though the results are influenced to some degree by demagnetization effects, the analysis method is robust and the parameters obtained from the fits to the single domain model reflect the variation of the physical parameters of the thin film stack. This means that field sweeps of the sensor response can be used to quantify the exchange and anisotropy fields as well as the magnetoresistive properties of the thin film stack.

5.2. Temperature Dependence of Parameters and Effect of Low-temperature Field Annealing

The studies on the as-deposited samples show that the effect of the low-temperature annealing is to decrease H_{ex} and H_K while $\Delta\rho/t$ remains essentially unchanged. The latter indicates that the microstructure of the stack is not significantly changed by the field annealing. The changes of H_{ex} and H_K indicate that the interaction between the ferromagnetic and antiferromagnetic layers is sensitive to the low-temperature field annealing. Considering the exchange bias as an interface phenomenon, the exchange bias field and the coupling energy per area J are related by $J = \mu_0 M_s t_{FM} H_{ex}$, where $\mu_0 M_s \approx 1.0$ T is the saturation flux density of permalloy and t_{FM} = 30 nm is the thickness of the permalloy layer. Inserting the values of H_{ex} from the VSM measurements in Table 1, we obtain J_{eb} = 0.07 mJ/m^2, which is comparable to values reported in the literature for similar stacks [8, 9].

The low-temperature annealing at 280 °C and 320 °C resulted in reductions of H_{ex} of 34 % and 52 %, respectively. Similar observations have been made in studies of similar structures with a top-pinned ferromagnet [8-11]. Previous studies have generally used measurements of the magnetic hysteresis by magnetometry [9-11], magnetooptical measurements [9] or Lorentz microscopy [8] to characterize the variation of H_{ex} and H_K with temperature, but they have not systematically studied the reversible and irreversible changes induced by exposure to elevated temperatures.

In this work we were able to separate reversible and irreversible changes of the parameters for the magnetic stack vs. temperature for samples exposed to different low-temperature field annealing conditions. We find that the temperature variation of $\Delta\rho/t$ is fully reversible. For the exchange bias field H_{ex} we find that the relative *reversible* change with temperature is the same for all samples (Fig. 5(a)). The *irreversible* change of H_{ex}, however, is sensitive to the field annealing and is significantly reduced compared to a sample without field annealing. For all field annealed samples, H_{ex} still shows irreversible change upon heating above 25 °C with a relative change that seems to be insensitive to the annealing conditions (Fig. 5(a)). For the anisotropy field H_K we find from Fig. 5(b) that both the reversible and irreversible changes upon exposure to elevated measuring temperatures are significant for the sample that was not field annealed, whereas the samples that were field annealed show significantly smaller changes with temperature. Only the sample annealed at 320 °C shows a negligible irreversible change of H_K upon exposure to 90 °C. The observed increase of the low-field sensitivity S_0 with field annealing and with exposure to elevated temperatures results from the combined effect of the reversible decrease of $\Delta\rho/t$ and the decrease of H_K+H_{ex} (cf. Eq. (6)), where the latter term dominates the temperature dependence.

To further investigate the effect of repeated exposure to elevated temperatures, we studied in Section 4.3 the samples with no annealing and with field annealing at 280 °C for repeated cycles between

90 °C and 25 °C. In Fig. 6(a), we found that for both the annealed and the un-annealed sample that the irreversible changes in the sensitivity as measured at 25 °C take place upon repeated exposure to 90 °C on a time scale of hours. Moreover, the relative change in sensitivity for the un-annealed sample is several times bigger than for the annealed sample. This change in sensitivity has to be attributed to the change in H_K and H_{ex}. Indeed, these two parameters show decay upon long exposure to 90 °C. Also, they show reduced irreversible changes in the annealed sensor compared to the un-annealed one.

For all samples, we find that even after field annealing at temperatures up to 320 °C, the values of H_{ex} and H_K still show irreversible changes upon exposure to temperatures above room temperature. These changes have to be taken into account when these stacks and sensors are used for sensing purposes in environments at elevated temperatures. The largest changes are found for the sample that was not field annealed and we have found that the field annealing significantly reduces the irreversible changes.

5.3. Possible Mechanisms

Several reports in the literature have studied the effect of annealing at low temperatures on the microstructure. King *et al.* [8] studied the magnetization reversal of NiFe/IrMn exchange bias couples by Lorentz transmission electron microscopy. For an un-annealed sample, they found that the magnetic domain structure in the ferromagnetic layer was highly complex on a microscopic scale near room temperature with no clear overall orientation. After field annealing of the sample at 300 °C, they found significantly larger magnetic domains that were essentially oriented along the cooling field. They could not detect any changes of the microstructure and therefore attributed the change of behavior to a reduction of the local pinning strength of the IrMn grains upon annealing. Thus, the IrMn grains strongly pinned the ferromagnetic layer before annealing resulting in the highly complex domain structure, but after annealing the pinning strength decreased due to relaxation in the spin structure of the IrMn grains such that the local pinning was insufficient to force the ferromagnet to orient along the local pinning field.

Geshev *et al.* [10] carefully studied the interface between Co and IrMn by high resolution cross-sectional TEM and X-ray reflectivity measurements and found no effect of annealing at 215 °C on the microstructure at the interface. Upon annealing in a magnetic field applied along the initial exchange bias direction they observed a clear reduction of H_{ex} that they attributed to relaxation of frustrated spins in the top IrMn layer. They hypothesized that the first few atomic layers of the IrMn layer show paramagnetic behavior and align themselves with the moments from the ferromagnet. When enough atomic layers of the IrMn film to sustain antiferromagnetic order are deposited, the competition between the alignment of the interface spins with those of the ferromagnetic layer and the antiferromagnetic ordering will result in high frustration of the spin structure of the IrMn layer near the interface and a high number of uncompensated spins at the interface, where the latter gives rise to the high initial exchange bias. The annealing enables relaxation of the spin structure resulting in a reduction of the pinning strength and hence of H_{ex}.

Our findings that irreversible changes of H_{ex} appear slightly above room temperature even for a sample annealed at 320 °C for one hour and that repeated exposure to elevated temperatures result in gradually decreasing values of H_{ex} indicate that a slow, thermally activated process is involved in the change of H_{ex} vs. time and temperature and that the number of uncompensated interfacial spins of the IrMn layer decreases as a result of the relaxation process. Thus, our observations are consistent with the above interpretation in terms of thermal relaxation of frustrated spins in the IrMn layer near the interface to the ferromagnet. We hope that our studies will provide further inspiration to further theoretical work on this interesting topic.

5. Conclusion

We have shown that measurements of the response vs. magnetic field of planar Hall effect Wheatstone bridges can be used to extract the exchange field H_{ex}, the anisotropy field H_K and the magnetoresistive properties of the exchange-biased stack of the sensors. We have studied the temperature variation of these parameters for a top-pinned NiFe/IrMn stack in the interval between 25 °C and 90 °C for samples that were not annealed and samples that were low-temperature field annealed at 240 °C, 280 °C and 320 °C for one hour. In our experiments we separated reversible and irreversible parameter changes. We found that the magnetoresistive effect is not significantly affected by the low-temperature field annealing and only shows reversible changes upon exposure to elevated temperatures. Both H_{ex} and H_K are sensitive to annealing as well as the exposure to elevated temperatures and the relative reversible decrease of H_{ex} with temperature can be described by a single temperature coefficient. Field annealing significantly reduces but does not eliminate the irreversible changes of both H_{ex} and H_K upon exposure to temperatures even slightly above room temperature. In experiments where both field annealed and un-annealed sensors were repeatedly exposed to 90 °C, we found a large initial change and a gradual reduction of the change upon further exposure. We take these observations as indicative of a slow thermally activated process that reduces the local pinning strength of the IrMn at the interface. The observations are consistent with previous interpretations in the literature in terms of thermal relaxation of frustrated spins in the antiferromagnet near the interface to the ferromagnet, but further work is required to firmly establish this hypothesis.

The present results have important consequences for the use of permalloy-IrMn exchange-bias couples in magnetic field sensors operating at variable temperatures. Stacks with no annealing are strongly influenced by exposure to temperatures above room temperature and these should thus be used with care in applications where the sensor is exposed to elevated temperatures and high accuracy is required. Examples of such applications could be magnetic biosensors operating at variable temperatures (e.g. for studies of biological interactions vs. temperature) and magnetic field sensors operating in variable temperature conditions. The presented method provides an attractive approach to quantitative characterization of the temperature-induced changes by exposure to given temperature conditions. We have shown that low-temperature field annealing and prolonged exposure to the highest operating temperature substantially reduces subsequent irreversible changes with increasing temperatures but also that it is difficult to completely eliminate irreversible changes of the sensor parameters. These therefore have to be considered for the use of the structures in sensing applications.

Acknowledgements

F.W. Østerberg acknowledges support by the Copenhagen Graduate School for Nanoscience and Nanotechnology (C:O:N:T) and the Knut and Alice Wallenberg (KAW) Foundation.

References

[1]. A. Persson *et al.*, Low-frequency noise in planar Hall effect bridge sensors, *Sensors and Actuators A: Physical,* 171, 2011, pp. 212-218.
[2]. C. Damsgaard *et al.*, Temperature effects in exchange-biased planar hall sensors for bioapplications, *Sensors and Actuators A: Physical*, 156, 2009, pp. 103-108.
[3]. B. Dalslet *et al.*, Bead magnetorelaxometry with an on-chip magnetoresistive sensor, *Lab Chip,* 11, 2011, pp. 296-302.
[4]. A. Henriksen *et al.,* Planar Hall effect bridge magnetic field sensors, *Appl. Phys. Lett.,* 97, 2010, 013507.
[5]. S. Blundell, Magnetism in condensed matter, Oxford master, *Oxford University Press*, 2001.
[6]. C. Damsgaard *et al.*, Exchange-biased planar Hall effect sensor optimized for biosensor applications,

J. Appl. Phys., 103, 2008, 07A302.

[7]. M. Donolato *et al*., Size-dependent effects in exchange-biased planar Hall effect sensor crosses, *J. Appl. Phys.,* 109, 2011, 064511.

[8]. J. King *et al*., Magnetization reversal of NiFe films exchange-biased by IrMn and FeMn, *J. Phys. D: Applied Physics*., 34, 2001, pp. 528-538.

[9]. J. Van Driel *et al*., Exchange biasing by $Ir_{19}Mn_{81}$: Dependence on temperature, microstructure and antiferromagnetic layer thickness, *J. Appl. Phys*., 88, 2000, pp. 975.

[10].J. Geshev *et al*. Role of the uncompensated interface spins in polycrystalline exchange-biased systems, *J. Phys. D: Applied Physics,* 44, 2011, 095002.

[11].A. Devasahayam *et al*., Magnetic, temperature, and corrosion properties of the NiFe/IrMn exchange couple, *J. Appl. Phys.,* 83, 1998, pp. 7216.

2012 Copyright ©, International Frequency Sensor Association (IFSA). All rights reserved.
(http://www.sensorsportal.com)

International Frequency Sensor Association (IFSA) Publishing

Digital Sensors and Sensor Systems: Practical Design

Sergey Y. Yurish

The goal of this book is to help the practicians achieve the best metrological and technical performances of digital sensors and sensor systems at low cost, and significantly to reduce time-to-market. It should be also useful for students, lectures and professors to provide a solid background of the novel concepts and design approach.

Book features include:

- Each of chapter can be used independently and contains its own detailed list of references
- Easy-to-repeat experiments
- Practical orientation
- Dozens examples of various complete sensors and sensor systems for physical and chemical, electrical and non-electrical values
- Detailed description of technology driven and coming alternative to the ADC a frequency (time)-to-digital conversion

Digital Sensors and Sensor Systems: Practical Design will greatly benefit undergraduate and at PhD students, engineers, scientists and researchers in both industry and academia. It is especially suited as a reference guide for practicians, working for Original Equipment Manufacturers (OEM) electronics market (electronics/hardware), sensor industry, and using commercial-off-the-shelf components

Formats: printable pdf (Acrobat) and print (hardcover), 419 pages

ISBN: 978-84-616-0652-8,
e-ISBN: 978-84-615-6957-1

http://sensorsportal.com/HTML/BOOKSTORE/Digital_Sensors.htm

International Frequency Sensor Association (IFSA) Publishing

Modern Sensors, Transducers and Sensor Networks

Sergey Y. Yurish, Editor

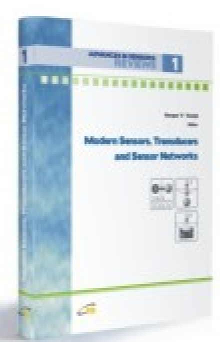

Modern Sensors, Transducers and Sensor Networks is the first book from the Advances in Sensors: Reviews book Series contains dozen collected sensor related state-of-the-art reviews written by 31 internationally recognized experts from academia and industry.

Built upon the series Advances in Sensors: Reviews - a premier sensor review source, the *Modern Sensors, Transducers and Sensor Networks* presents an overview of highlights in the field. Coverage includes current developments in sensing nanomaterials, technologies, MEMS sensor design, synthesis, modeling and applications of sensors, transducers and wireless sensor networks, signal detection and advanced signal processing, as well as new sensing principles and methods of measurements.

Modern Sensors, Transducers and Sensor Networks is intended for anyone who wants to cover a comprehensive range of topics in the field of sensors paradigms and developments. It provides guidance for technology solution developers from academia, research institutions, and industry, providing them with a broader perspective of sensor science and industry.

Formats: printable pdf (Acrobat) and print (hardcover), 422 pages

ISBN: 978-84-615-9613-3,
e-ISBN: 978-84-615-9012-4

http://sensorsportal.com/HTML/BOOKSTORE/Advance_in_Sensors.htm

Guide for Contributors

Aims and Scope

Sensors & Transducers Journal (ISSN 1726-5479) provides an advanced forum for the science and technology of physical, chemical sensors and biosensors. It publishes state-of-the-art reviews, regular research and application specific papers, short notes, letters to Editor and sensors related books reviews as well as academic, practical and commercial information of interest to its readership. Because of it is a peer reviewed international journal, papers rapidly published in *Sensors & Transducers Journal* will receive a very high publicity. The journal is published monthly as twelve issues per year by International Frequency Sensor Association (IFSA). In additional, some special sponsored and conference issues published annually. *Sensors & Transducers Journal* is indexed and abstracted very quickly by Chemical Abstracts, IndexCopernicus Journals Master List, Open J-Gate, Google Scholar, etc. Since 2011 the journal is covered and indexed (including a Scopus, Embase, Engineering Village and Reaxys) in Elsevier products.

Topics Covered

Contributions are invited on all aspects of research, development and application of the science and technology of sensors, transducers and sensor instrumentations. Topics include, but are not restricted to:

- Physical, chemical and biosensors;
- Digital, frequency, period, duty-cycle, time interval, PWM, pulse number output sensors and transducers;
- Theory, principles, effects, design, standardization and modeling;
- Smart sensors and systems;
- Sensor instrumentation;
- Virtual instruments;
- Sensors interfaces, buses and networks;
- Signal processing;
- Frequency (period, duty-cycle)-to-digital converters, ADC;
- Technologies and materials;
- Nanosensors;
- Microsystems;
- Applications.

Submission of papers

Articles should be written in English. Authors are invited to submit by e-mail editor@sensorsportal.com 8-14 pages article (including abstract, illustrations (color or grayscale), photos and references) in both: MS Word (doc) and Acrobat (pdf) formats. Detailed preparation instructions, paper example and template of manuscript are available from the journal’s webpage: http://www.sensorsportal.com/HTML/DIGEST/Submition.htm Authors must follow the instructions strictly when submitting their manuscripts.

Advertising Information

Advertising orders and enquires may be sent to sales@sensorsportal.com Please download also our media kit: http://www.sensorsportal.com/DOWNLOADS/Media_Kit_2012.pdf

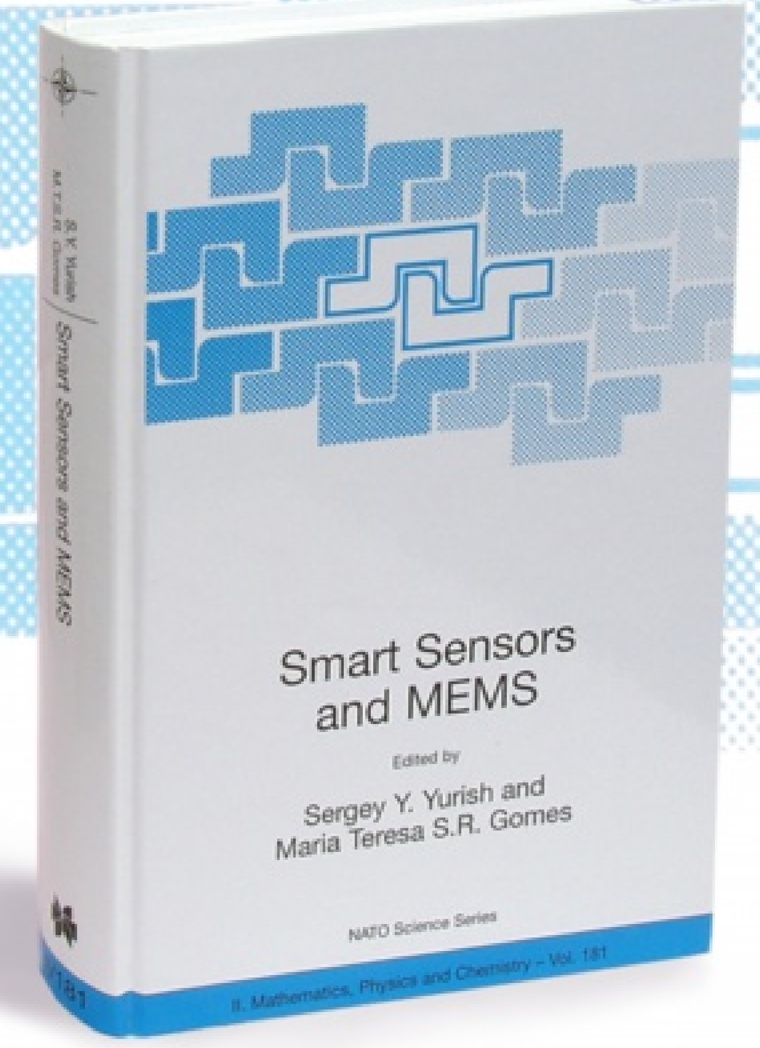

Smart Sensors and MEMS

Edited by

Sergey Y. Yurish and
Maria Teresa S.R. Gomes

The book provides an unique collection of contributions on latest achievements in sensors area and technologies that have made by eleven internationally recognized leading experts ...and gives an excellent opportunity to provide a systematic, in-depth treatment of the new and rapidly developing field of smart sensors and MEMS.

The volume is an excellent guide for practicing engineers, researchers and students interested in this crucial aspect of actual smart sensor design.

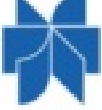

Kluwer Academic Publishers

Order online:
www.sensorsportal.com/HTML/BOOKSTORE/Smart_Sensors_and_MEMS.htm

www.sensorsportal.com